Physics Letters B 703 (2011) 547–551

Contents lists available at ScienceDirect

Physics Letters B

www.elsevier.com/locate/physletb

Comparative results on collimation of the SPS beam of protons and Pb ions with bent crystals

W. Scandale [a,b,f], G. Arduini [a], R. Assmann [a], C. Bracco [a], F. Cerutti [a], J. Christiansen [a], S. Gilardoni [a], E. Laface [a], R. Losito [a], A. Masi [a], E. Metral [a], D. Mirarchi [a], S. Montesano [a], V. Previtali [a], S. Redaelli [a], G. Valentino [a], P. Schoofs [a], G. Smirnov [a], L. Tlustos [a], E. Bagli [c], S. Baricordi [c], P. Dalpiaz [c], V. Guidi [c], A. Mazzolari [c], D. Vincenzi [c], S. Dabagov [d], F. Murtas [d], A. Carnera [e], G. Della Mea [e], D. De Salvador [e], A. Lombardi [e], O. Lytovchenko [e], M. Tonezzer [e], G. Cavoto [f], L. Ludovici [f], R. Santacesaria [f], P. Valente [f], F. Galluccio [g], A.G. Afonin [h], M.K. Bulgakov [h], Yu.A. Chesnokov [h], V.A. Maisheev [h], I.A. Yazynin [h], A.D. Kovalenko [i], A.M. Taratin [i,*], V.V. Uzhinskiy [i], Yu.A. Gavrikov [j], Yu.M. Ivanov [j], L.P. Lapina [j], V.V. Skorobogatov [j], W. Ferguson [k], J. Fulcher [k], G. Hall [k], M. Pesaresi [k], M. Raymond [k], A. Rose [k], M. Ryan [k], O. Zorba [k], G. Robert-Demolaize [l], T. Markiewicz [m], M. Oriunno [m], U. Wienands [m]

[a] CERN, European Organization for Nuclear Research, CH-1211 Geneva 23, Switzerland
[b] Laboratoire de l'Accelerateur Lineaire (LAL), Universite Paris Sud Orsay, Orsay, France
[c] INFN Sezione di Ferrara, Dipartimento di Fisica, Universitá di Ferrara, Ferrara, Italy
[d] INFN LNF, Via E. Fermi, 40 00044 Frascati, Rome, Italy
[e] INFN Laboratori Nazionali di Legnaro, Viale Universitá 2, 35020 Legnaro (PD), Italy
[f] INFN Sezione di Roma, Piazzale Aldo Moro 2, 00185 Rome, Italy
[g] INFN Sezione di Napoli, Italy
[h] Institute of High Energy Physics, Moscow Region, 142284 Protvino, Russia
[i] Joint Institute for Nuclear Research, Joliot-Curie 6, 141980 Dubna, Moscow Region, Russia
[j] Petersburg Nuclear Physics Institute, 188300 Gatchina, Leningrad Region, Russia
[k] Imperial College, London, United Kingdom
[l] Brookhaven National Laboratories, P.O. Box 5000, Upton, NY 11973-5000, USA
[m] SLAC National Accelerator Laboratory, 2575 Sand Hill Road, Menlo Park, CA 94025, USA

ARTICLE INFO

Article history:
Received 29 June 2011
Received in revised form 15 July 2011
Accepted 10 August 2011
Available online 16 August 2011
Editor: L. Rolandi

Keywords:
Accelerator
Beam collimation
Crystal
Channeling

ABSTRACT

New experiments on crystal assisted collimation have been carried out at the CERN SPS with stored beams of 120 GeV/c protons and Pb ions. Bent silicon crystals of 2 mm long with about 170 μrad bend angle and a small residual torsion were used as primary collimators. In channeling conditions, the beam loss rate induced by inelastic interactions of particles with the crystal nuclei is minimal. The loss reduction was about 6 for protons and about 3 for Pb ions. Lower reduction value for Pb ions can be explained by their considerably larger ionization losses in the crystal. In one of the crystals, the measured fraction of the Pb ion beam halo deflected in channeling conditions was 74%, a value very close to that for protons. The intensity of the off-momentum halo leaking out from the collimation station was measured in the first high dispersion area downstream. The particle population in the shadow of the secondary collimator–absorber was considerably smaller in channeling conditions than for amorphous orientations of the crystal. The corresponding reduction was in the range of 2–5 for both protons and Pb ions.

1. Introduction

The collimation system of a hadron collider such as the Large Hadron Collider (LHC) is a multi-stage system. A primary collimator manufactured from a heavy solid material deflects halo particles by multiple Coulomb scattering thus increasing their impact parameters on encounters with a secondary collimator–absorber. If a bent crystal were to be used as a primary collimator, halo particles deflected due to channeling along the crystal planes should hit the absorber far from its edge. As a result the possibility of secondary scattering from the absorber back into the beamline should be drastically reduced so that the collimation efficiency would be significantly increased.

* Corresponding author.
E-mail address: alexander.taratin@cern.ch (A.M. Taratin).

0370-2693/$ – see front matter
doi:10.1016/j.physletb.2011.08.023

Fig. 1. (Color online.) The modified layout of the UA9 experiment. The primary collimators — bent crystals C1–C4 are located upstream the quadrupole QF518 (QF1). The TAL acting as a secondary collimator–absorber is upstream the quadrupole QF 520 (QF2). The TAL2 station in a high dispersion area is used to measure off-momentum particles produced in the collimation process.

Experiments on beam halo collimation with short bent crystals have already been performed at the IHEP synchrotron [1], RHIC [2] and Tevatron [3]. The possibility to increase significantly the collimation efficiency of the LHC beam halo using a crystal primary collimator has been studied in simulation [4]. A possible layout for crystal-assisted collimation at the LHC has been considered in [5].

In 2009, the UA9 Collaboration started investigating crystal assisted collimation at the CERN Super Proton Synchrotron (SPS) using a bent silicon crystal as a primary collimator and a tungsten absorber as a secondary collimator. The first UA9 results with 120 GeV/c stored proton beams were reported in [6]. Perfect alignment of the crystal to achieve deflection of halo particles due to channeling could be obtained quickly and is easily reproducible. The channeling efficiency of halo protons measured by intercepting the deflected beam with another collimator was 75% and 85% for two crystals tested. The efficiency was determined as the ratio of the beam halo fraction deflected by the bend angle due to channeling to the whole fraction which hit the absorber. A visual image of the deflected beam was observed with a MEDIPIX pixel detector [7]. The halo loss rate due to inelastic nuclear interactions of protons in the aligned crystal was found to be about five times smaller than for its amorphous orientation. Although the channeling efficiency P_{ch} and the beam loss reduction in the aligned crystal R_{in} reported in [6] are large, they are smaller than expected. According to simulations one should find $P_{\mathrm{ch}} \approx 95\%$ and $R_{\mathrm{in}} \approx 36$. In [6] the discrepancy between the experimental results and predictions was supposed to be caused by torsion of the used crystal, known to be larger than 10 μrad/mm, which causes different orientations of the crystal planes at different vertical positions of the beam.

As also reported in [6] the beam loss measurements in regions of the SPS ring far from the collimation area have shown a reduction by only 30% for an aligned crystal with respect to its amorphous orientation. This ratio, significantly smaller than predicted by simulation, was considered unreliable since during the data taking the stored beam intensity of $0.5\text{–}5 \times 10^{10}$ particles was in a range in which the SPS beam loss monitors around the ring are known to be noisy and to lack sensitivity. For this reason, an additional measuring station with an adjustable aperture restriction was installed at the first accelerator location with high dispersion downstream of the crystal-absorber area to improve the situation for measuring the off-momentum particle leakage.

In this Letter the UA9 experimental results on the SPS beam collimation obtained in a modified layout with new low torsion bent crystals are presented. The experiments have been performed with stored proton and Pb ion beams with the same momentum of 120 GeV/c per charge. It should be noted that the first experiment on the extraction of the SPS beam of Pb ions was performed with a 40 mm long bent silicon crystal [8]. The observed extraction efficiency was about 10%.

2. The experiment description

Fig. 1 shows the schematic layout of the UA9 experiment, recently improved with respect to the earlier version in [6]. The primary collimator and the absorber stations are installed at SPS azimuths with relative horizontal betatron phase advance close to 90 degrees and with a large value of the horizontal beta function. They sit upstream of the quadrupoles QF518 and QF520 (marked as QF1 and QF2 in Fig. 1), respectively. The first station now contains four crystals C1–C4, which can each be used separately as a primary collimator. Two new crystals C3 and C4 are installed in a new goniometer constructed and produced by IHEP with an angular accuracy of about ±10 μrad (four times better than the accuracy of the goniometers supporting the crystals C1 and C2). The parameters of C3 (quasi-mosaic) and C4 (strip) crystals produced according to the technologies described in [9–11] are presented in Table 1. The second station contains a 60 cm long tungsten absorber TAL used as a secondary collimator. A MEDIPIX-type detector MED with square 55×55 μm^2 pixels was used to obtain on-line images of the deflected beam. The two-sided LHC collimator prototype COL was used for the alignment of the UA9 devices relative to the beam orbit. The BLMs are low noise, high sensitivity prototypes, specially developed for LHC [12].

Table 1
Crystal parameters.

Crystal	Length (mm)	Bend angle (μrad)	Torsion (μrad/mm)	Miscut angle (μrad)
C3	2.1	165	1	90
C4	2.0	176	0.6–1.0	200

Table 2
Relevant accelerator parameters.

Parameter	C3	COL	TAL	SC
β_x (m)	73.496	24.472	88.601	89.688
σ_x (mm)	1.1	0.635	1.21	1.216
$\Delta\mu_x$ from C3 (2π)	0	0.1657	0.247	0.4884
D_x (m)	−0.8084	−0.2470	−0.0393	3.4138

Off-momentum particles with $\delta = p/p_o - 1 \neq 0$ (p and p_o are momenta of a circulating particle and of the synchronous particle, respectively) produced in the crystal or in the absorber and escaping from the collimation area have large displacements from the orbit at high dispersion azimuths, $x_\delta = D_x\delta$, where D_x is the value of the dispersion function. A new station, called TAL2 in Fig. 1, with targets limiting the accelerator aperture was installed in the high dispersion area downstream the collimator–absorber for an optimal detection of the surviving off-momentum halo. The station consists of a beam scraper SC (a 10 cm long bar of duralumin), a movable Cherenkov detector CH and the beam loss monitors (BLM).

In the SPS, protons or Pb ion beams of a few 10^{10} particles were accelerated to 120 GeV/c per charge with nominal betatron tunes $Q_{\mathrm{H}} = 26.13$ and $Q_{\mathrm{V}} = 26.18$. The horizontal RMS emittance was about $\varepsilon = 0.016$ μm rad. The relevant accelerator parameters at the azimuths of some UA9 elements are listed in Table 2, where β_x is the value of the horizontal beta-function, σ_x is the RMS value of the horizontal beam size and $\Delta\mu_x$ is the horizontal phase advance between the elements.

At the beginning of each measurement the LHC collimator prototype was centered relative to the closed orbit. The collimator half gap $X_{1/2}$ determined the reference beam envelope. Then the align-

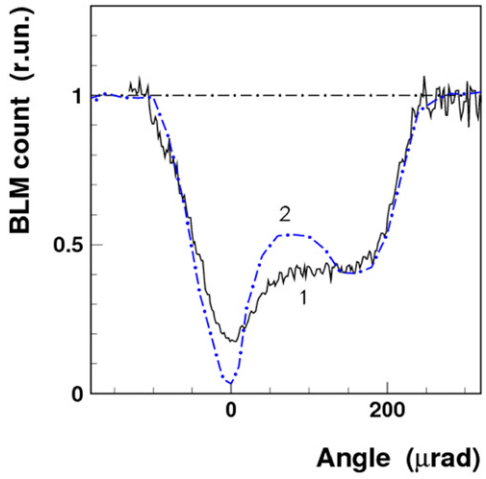

Fig. 2. (Color online.) Proton beam. (1) The dependence of the beam loss monitor signal on the angular position of the crystal 3 normalized to its value for the amorphous orientation of the crystal (dot-dashed line). (2) The dependence of the number of inelastic nuclear interactions of protons in a perfect crystal on its orientation angle obtained by simulation.

ment positions for all UA9 movable elements were determined by fixing their positions at the edge of the LHC collimator shadow. After the alignment almost all elements were moved back to their garage positions while one of the crystals and the TAL were put in the collimation positions. The crystal under test was moved closer to the beam and the TAL moved further away from the orbit improving conditions for the multi-turn extraction of halo particles.

3. Experimental results

We first consider the results obtained with an SPS stored beam of protons using a new crystal (C3). Beam losses in the crystal are detected using the BLM downstream of the crystal station as a function of the crystal orientation. The observed dependence of the BLM signal is normalized to its value for amorphous orientation of the crystal.

In Fig. 2 curve 1 shows the observed dependence of beam losses on the angular position of C3 when its distance from the orbit was $X_{C3} = 7.6$ mm ($6.9\sigma_x$) and the distance of the TAL was $X_{TAL} = 10.1$ mm ($8.3\sigma_x$). The BLM signal is reduced by a factor $R_{in} \approx 6$ when the direction of the crystal planes at the entrance face is close to the beam envelope direction (left minimum in Fig. 2). For these crystal orientations, halo protons deflected due to channeling in the crystal hit the TAL in the same turn and inelastic nuclear interactions can occur in the crystal only for the small non-channeled fraction of the halo. Curve 2 in Fig. 2 shows the dependence of inelastic nuclear losses of protons on crystal orientation obtained by simulation based on the model described in [13] taking into account synchrotron oscillations of particles. The loss reduction for the channeling position obtained in the simulation is about 30. The beam loss reduction observed in the present experiments is a little larger than in earlier results reported in [6] but considerably smaller than the predicted value. This discrepancy cannot be caused by the crystal torsion because its value for new crystals is significantly smaller than the critical angle ($\theta_c \approx 20$ μrad).

Table 3 shows the values of the channeling efficiency and inelastic interaction probability for a few orientation angles near perfect crystal alignment obtained by simulation. The parameter changes relative to the value for perfect alignment are also shown. The channeling efficiency reduces a little whereas the beam loss increase is more than 40 times larger. These data clearly demonstrate that the measurement of beam halo losses in the crystal is a very sensitive method for the crystal collimation studies.

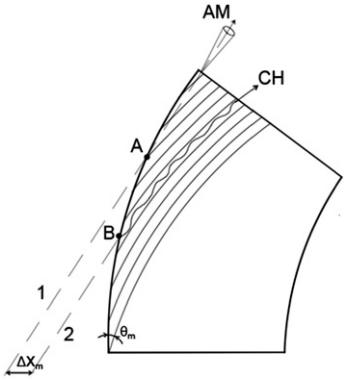

Fig. 3. (Color online.) The crystal with a miscut angle θ_m between its surface and crystallographic planes and trajectories of a halo particle at the first (1) and second (2) hits with the crystal. In both cases the particle enters the crystal through its side face. The particle obtains a small amplitude increase Δx_m due to Coulomb scattering in the first passage and in the second encounter its direction is tangential to the shortened planes. Therefore, it can be captured and deflected by these shortened channels.

Table 3
Channeling efficiency and beam loss probability.

θ_o (μrad)	P_{ch} (%)	$\Delta P_{ch}/P_{ch}(0)$ (%)	P_{in} (%)	$\Delta P_{in}/P_{in}(0)$ (%)
10	88.7	−4	1.02	178
0	92.4	0	0.367	0
−10	91.4	−1.1	0.538	46.6

The angular region with reduced counts on the right of the channeling minimum in Fig. 2 is an expected consequence of volume reflection (VR) of protons from bent planes in the crystal. The angular range of VR is about equal to the crystal bend angle, i.e. 165 μrad. Particles deflected due to VR perform a smaller number of passages through the crystal to reach the TAL aperture than for amorphous orientations of the crystal. However, beam losses observed in VR mode are considerably smaller than the simulation results.

The discrepancies in the beam losses observed for channeling and VR areas of the crystal orientation may be caused by the existence of the miscut angle between the crystal surface and the crystallographic planes appearing as a result of the crystal sample production from a silicon ingot. The effect of the crystal miscut was previously considered in the first extraction experiment of the SPS proton beam [14]. The miscut angle values for crystal 3 and 4 are given in Table 1.

Possible situations for VR and channeling crystal orientations discussed below may explain how a crystal miscut could affect the beam loss rate. Quantitative considerations to support such an explanation should be based on a simulation model of the crystal miscut not yet available. Fig. 3 shows schematically a crystal with a miscut angle θ_m for its VR orientation and possible trajectories of a halo particle in two subsequent passages. The first encounter with the crystal occurs at the point A of its lateral face because of a small impact parameter of the particle. It gives rise to a small amplitude increase Δx_m due to Coulomb scattering in its first passage through the crystal as in amorphous matter. At the next hit the particle may enter the crystal again through its lateral face at the point B in a direction already tangential to the shortened planes. As a result the particle is captured and deflected by the shorter channels. Such a mechanism should reduce the number of turns to

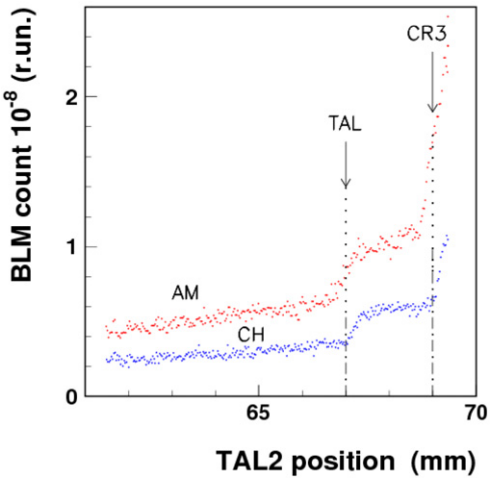

Fig. 4. (Color online.) Proton beam. The dependence of the beam loss monitor signal normalized to the beam intensity on the horizontal position of the scraper (Sc) in a high dispersion area behind the collimator–absorber during the scraper scan from the beam periphery towards the orbit for the crystal 3 in the amorphous (AM) and channeling (CH) orientations. The projections of the TAL and the crystal 3 positions are shown by the arrows.

extract the halo particles and consequently the beam losses for VR crystal orientations.

The situation for channeling orientations is similar. It can be realized by a small clockwise rotation of the crystal shown in Fig. 3. In this case a halo particle with a small impact parameter should also have the first encounter with the lateral face of the crystal where its momentum direction is far from the crystal plane direction. Passing through a large part of the crystal length the particle is deflected by multiple Coulomb scattering and on the following turns it hits the front face of the crystal where it may be captured into channeling and deflected by the full bend angle. The first passage through the crystal as in amorphous substance increases the probability of inelastic nuclear interactions for this halo fraction. Thus, the effect of the crystal miscut may at least partly explain both an increase of beam losses for channeling orientations and the opposite effect for VR.

The off-momentum fraction of beam halo particles escaping from the collimation area was estimated by using the scraper of the TAL2 station. Scans are usually made from the garage position to the location of the crystal edge projection calculated using the beta-function values. Fig. 4 shows the dependence of the BLM count on the horizontal position of the scraper during two of such scans performed for the crystal in the amorphous and channeling orientations. The measurements were made in the same SPS fill during contiguous time periods. The two arrows indicate the projected inner-edge positions of the TAL-absorber and crystal C3 at the TAL2-scraper azimuth, respectively. We conventionally define the off-momentum collimation leakage as the integral of the number of particles behind the TAL shadow, which can be lost somewhere in the SPS ring outside of the absorber. For the results reported here, the absorber shadow population for the well-aligned crystal was reduced by a factor of about 2 in comparison with the amorphous orientation. The observed reduction was larger, achieving about a factor 5, in similar measurements for some other experimental runs.

The experiments on the crystal collimation of the SPS stored beam of Pb ions were performed in a similar way. Scattering by inner electric field of a crystal for protons and Pb ions with the same momentum per charge (p/Z) is the same because it depends on this ratio. Therefore, the crystal channeling characteristics are the same for protons and Pb ions. The main differences compared

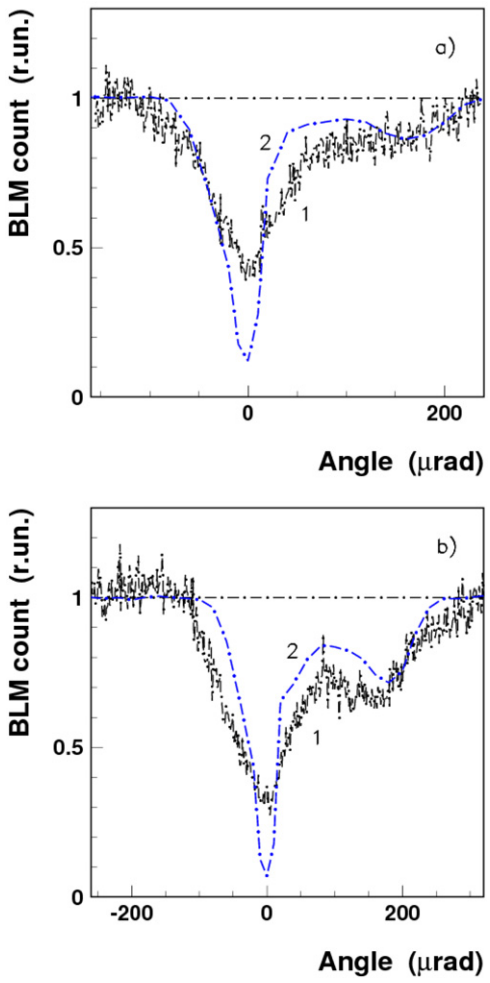

Fig. 5. (Color online.) Pb ion beam. (1) The dependences of the beam loss monitor signal on the angular position of the crystal 3 (a) and 4 (b) normalized to its value for the amorphous orientation of the crystal (dot-dashed line). (2) The simulation results for the number of inelastic nuclear interactions in the crystals.

to protons were caused by the strong increase of ionization losses and nuclear interaction cross sections for Pb ions in the crystal. In a 2 mm long silicon crystal in amorphous orientation the mean energy loss for protons is $\Delta E_{\mathrm{p}} = 1.05$ MeV and for Pb ions $\Delta E_{\mathrm{Pb}} = 6.59$ GeV. These values correspond to relative momentum deviations $\delta_{\mathrm{p}} = -8.7 \times 10^{-6}$ and $\delta_{\mathrm{Pb}} = -0.66 \times 10^{-3}$. During the data taking the SPS bucket half-height was $\delta_{\mathrm{h}} = 1.54 \times 10^{-3}$. Therefore, on average three passages of Pb ions through the nonaligned crystal were sufficient for their debunching. Moreover, the particle energy losses considerably increase their betatron oscillation amplitudes because of the orbit shift. The total cross section of Pb ion beam attenuation in silicon, which includes inelastic nuclear interactions and electromagnetic dissociation, was calculated according to the methods reported in [15–17], which describe well the existing experimental data. Its value $\sigma_{\mathrm{tot}} = \sigma_{\mathrm{h}} + \sigma_{\mathrm{ed}} = 4.323 + 1.091 = 5.414$ b is 10 times larger than for protons. The attenuation length equals 3.76 cm, therefore more than 5% of Pb ions will be lost in the passage through the non-aligned crystal.

Curve 1 in Figs. 5(a) and (b) shows the Pb ion beam losses as function of the orientation angle for crystal 3 (a) and crystal 4 (b). The simulation results for the number of Pb ion inelastic interactions in the crystals are shown by curve 2. When crystal 3 was used as a primary collimator the distances from the orbit were $X_{\mathrm{CR3}} = 5.8$ mm $(5.7\sigma_x)$ and $X_{\mathrm{TAL}} = 10.4$ mm $(9.3\sigma_x)$. The beam

halo losses were reduced by only 16% for VR orientations and by about 60% in channeling conditions that is a loss reduction factor $R_{\rm in} \approx 2.5$. The decrease of $R_{\rm in}$ for Pb ions in comparison with protons is caused by a considerably larger increase of betatron oscillation amplitudes for the particles which passed through the nonaligned crystal due to their larger energy losses. As a result, Pb ions more quickly reach the TAL. In the case of crystal 4 the distances from the orbit were $X_{\rm CR3} = 3$ mm (about $3\sigma_x$) and $X_{\rm TAL} = 7.9$ mm ($6.7\sigma_x$). The beam loss reduction in channeling conditions was considerably larger than for crystal 3, $R_{\rm in} \approx 3.5$.

A larger reduction of beam losses was also observed for VR orientations. In addition, a second minimum in the VR orientation region is clearly seen here. This minimum is observed for crystal orientations where the whole angular arc of the bent crystal planes is already on the same side relative to the beam envelope direction. Therefore, VR angular kicks always increase the particle oscillation amplitudes. The observed beam losses in channeling conditions are larger for crystal 3 than for crystal 4 because its deflecting planes are the (111) ones, which are non-equidistant. The channel width ratio is 3. The width of narrow channels is about 2.5 times smaller than for the (110) channels. Particles quickly dechannel from these narrow channels increasing the probability of inelastic interactions with the crystal nuclei. So, according to simulations, the probability of nuclear interactions in a single passage for parallel beam is 20% larger for crystal 3 than for crystal 4 with its (110) equidistant planes. The loss reduction factors for perfect crystal alignment obtained in our simulations are $R_{\rm in} = 8.3$ and 14.2 for crystal 3 and 4, respectively. For Pb ions there is the same character of discrepancies as for protons between the experimental and simulation values of beam losses in channeling and VR areas of the crystal orientations, which may also be explained by the crystal miscut effect.

The Pb ion beam halo fraction deflected due to channeling by the crystal 3 was measured by intersecting the deflected beam with the LHC prototype collimator as was done in the case of the proton beam collimation [6]. Its value was found to be 74%. The off-momentum Pb ion fraction generated in the collimation process was also measured by scanning the beam periphery in the TAL2 station with Cherenkov detector. The reduction factor up to 5 for the population of particles in the collimator–absorber shadow was observed.

4. Conclusions

Recent results of UA9 experiments on crystal collimation at the CERN SPS show that in the case of Pb ions the beam halo can also be efficiently deflected onto the secondary collimator–absorber with a bent crystal. The extraction efficiency of Pb ions from the circulating beam halo measured for one of the crystals was 74%. The crystal alignment was easily found through the reduction of beam losses in the crystal, which were about 6 for protons and about 3 for Pb ions. The smaller loss reduction for Pb ions, compared to protons, is caused by their larger ionization losses. As a result, their oscillation amplitudes increase considerably in the passages through the nonaligned crystal and they more quickly reach the absorber.

The simulation results qualitatively describe well the angular dependence of beam losses in the crystal. The quantitative discrepancies remaining in spite of the low torsion of new crystals used for the present experiments may be caused by the influence of the crystal miscut. It should be made much smaller than the crystal bend angle to reduce its effect.

A scan of horizontal positions performed in the high dispersion area behind the absorber showed that the beam tail in the shadow of the absorber populated by off-momentum particles produced in the collimation process was reduced by a factor of 2–5 for perfect crystal alignment in comparison with its amorphous orientation.

It should be noted that damage to the crystal irradiated by high energy heavy ions should be considerably larger than by protons. Therefore, it is important to perform a study of the crystal radiation resistance with high energy heavy ion beams as was done with protons in [18] to estimate the possibility of using a crystal primary collimator also for the LHC ion beams.

Acknowledgements

We wish to acknowledge the strong support of the EN-STI and BE-AOP groups. We also acknowledge the partial support by the Russian Foundation for Basic Research Grants 05-02-17622 and 06-02-16912, the RF President Foundation Grant SS-3383.2010.2, the “LHC Program of Presidium of Russian Academy of Sciences” and the grant RFBR-CERN 08-02-91020. G.C. and R.S. acknowledge the support from MIUR (grant FIRB RBFR085M0L_001/I11J10000090001 and PRIN 2008TMS4ZB). Work supported by the EuCARD program GA 227579, within the “Collimators and Materials for high power beams” work package (Colmat-WP). The Imperial College group gratefully acknowledges support from the UK Science and Technology Research Council. US participants supported by US DOE under the LHC Accelerator Research Program (LARP).

References

[1] A.G. Afonin, et al., Phys. Rev. Lett. 87 (2001) 094802.
[2] R.P. Fliller, et al., Nucl. Instrum. Methods B 234 (2005) 47.
[3] R.A. Carrigan Jr., et al., Fermilab-CONF-06-309-AD.
[4] V.M. Biryukov, V.N. Chepegin, Yu.A. Chesnokov, V. Guidi, W. Scandale, Nucl. Instrum. Methods B 234 (2005) 23.
[5] R. Assmann, S. Redaelli, W. Scandale, in: EPAC Proceedings, Edinburgh, 2006, p. 1526.
[6] W. Scandale, et al., Phys. Lett. B 692 (2010) 78.
[7] X. Llopart, et al., IEEE Trans. Nuclear Sci. 49 (2002) 2279.
[8] G. Arduini, et al., Phys. Rev. Lett. 79 (1997) 4182.
[9] Yu.M. Ivanov, A.A. Petrunin, V.V. Skorobogatov, JETP Lett. 81 (2005) 99.
[10] S. Baricordi, et al., Appl. Phys. Lett. 91 (2007) 061908.
[11] S. Baricordi, et al., J. Phys. D: Appl. Phys. 41 (2008) 245501.
[12] E.B. Holzer, et al., in: Proceedings of HB2010, Morschach, Switzerland, CERN-BE-2010-031, p. 1.
[13] W. Scandale, A. Taratin, CERN report CERN/AT 2008-21.
[14] K. Elsener, et al., Nucl. Instrum. Methods B 119 (1996) 215.
[15] S.Yu. Shmakov, V.V. Uzhinskii, A.M. Zadorozgny, Comput. Phys. Commun. 54 (1989) 125.
[16] V.M. Grichine, Nucl. Instrum. Methods B 267 (2009) 2460.
[17] F. Ballarini, G. Battistoni, F. Cerutti, et al., Nuclear models in FLUKA: present capabilities, open problems and future improvements, preprint SLAC-PUB-10813, October 2004.
[18] A. Baurichter, et al., Nucl. Instrum. Methods B 119 (1996) 172.